JOURNAL OF VIROLOGY, May 2008, p. 4371–4383 Vol. 82, No. 9
0022-538X/08/$08.00+0 doi:10.1128/JVI.02027-07

Infectious Spleen and Kidney Necrosis Virus ORF48R Functions as a New Viral Vascular Endothelial Growth Factor▽

Zi-Liang Wang,[1]† Xiao-Peng Xu,[1]† Bai-Liang He,[1] Shao-Ping Weng,[1] Jia Xiao,[1] Li Wang,[1] Ting Lin,[1] Xi Liu,[1] Qing Wang,[1] Xiao-Qiang Yu,[2] and Jian-Guo He[1]*

State Key Laboratory for Biocontrol, School of Life Sciences, Sun Yat-sen (Zhongshan) University, 135 Xingang Road West, Guangzhou 510275, People's Republic of China,[1] and Division of Cell Biology and Biophysics, School of Biological Sciences, University of Missouri—Kansas City, Kansas City, Missouri 64110[2]

Received 13 September 2007/Accepted 1 February 2008

Infectious spleen and kidney necrosis virus **(ISKNV) causes a pandemic and serious disease in fish. Infection by ISKNV causes epidermal lesions, in which petechial hemorrhages and abdominal edema are prominent features. ISKNV ORF48R contains a domain similar to that of the platelet-derived growth factor and vascular endothelial growth factor (VEGF) families of proteins. ISKNV ORF48R showed higher similarity to the VEGFs encoded by *Megalocytivirus* and *Parapoxvirus* than to those encoded in fish and mammals. We used zebrafish as a model and constructed a recombinant plasmid containing the DNA sequence of ISKNV ORF48R to study ISKNV infection. The plasmid was microinjected into zebrafish embryos at the one-cell stage. Overexpression of the ISKNV ORF48R gene results in pericardial edema and dilation at the tail region of zebrafish embryos, suggesting that ISKNV ORF48R induces vascular permeability. ISKNV ORF48R is also able to stimulate a striking expression of *flk1* in the zebrafish dorsal aorta and the axial vein. Furthermore, ISKNV ORF48R, while cooperating with zebrafish $VEGF_{121}$, can stimulate more striking expression of *flk1* than can either ISKNV ORF48R or zebrafish $VEGF_{121}$ alone. However, decreased expression of FLK-1 by gene knockdown results in the disappearance of pericardial edema and dilation at the tail region of zebrafish embryos induced by overexpression of ISKNV ORF48R in the early stages of embryonic development.**

Vascular endothelial growth factor (VEGF) functions as a specific mitogen for vascular endothelial cells and a potent inducer of vascular permeability. Members of the VEGF family play an important role in vasculogenesis during embryogenesis (16, 17, 60, 66) and in angiogenesis during adulthood. The latter is related to wound healing and some pathological conditions including tumor formation and inflammatory conditions (4, 40, 58, 61). The mammalian VEGF family is composed of VEGFs (VEGF-A, VEGF-B, VEGF-C, and VEGF-D) and placenta growth factors (PlGFs), which are secreted, homodimeric glycoproteins that share 30 to 45% identity in their amino acid sequence. The VEGF family members exert their biological activities via a family of tyrosine kinase receptors, including VEGF receptor 1 (VEGFR-1), VEGFR-2, and VEGFR-3 (1, 18, 51, 78). VEGFR-1 is expressed by endothelial and hematopoietic cells and plays a vital role in differentiation and recruitment of these cells via VEGF-A, VEGF-B, and PlGF. VEGFR-1 is also involved in the induction of proinflammatory cytokine production (26, 45, 72). VEGFR-2 is the primary signaling receptor that has functions in endothelial cell proliferation, migration, and vascular permeability activated by VEGF-A, VEGF-C, and VEGF-D. VEGFR-3, bound with VEGF-C and VEGF-D, is involved in the regulation of the lymphatic vasculature (47). In addition, the neuronal cell guidance receptors, neuropilin 1 and neuropilin 2, have been shown to interact with VEGF-A, VEGF-B, VEGF-C, and PlGF and to act as coreceptors to enhance their binding of VEGFRs (47, 49, 67).

Besides mammalian VEGFs, a group of parapoxvirus-derived homologues of VEGF, collectively designated VEGF-E, have been reported (42, 46, 48, 76). The genus *Parapoxvirus* includes *Orf virus* (ORFV) (19, 22), *Pseudocowpox virus* (PCPV) (27, 68), *Bovine papular stomatitis virus* (BPSV) (39), and *Parapoxvirus of red deer in New Zealand* (PVNZ) (69). These viruses usually infect the muzzle or teats of sheep, goats, and cattle (22, 27, 39, 69). They can also readily infect humans. The lesions that result from these viral infections are characterized by vascular dilation, dermal edema, and proliferation of endothelial cells (43, 55). The presence of the VEGF homologue in the virus provides a probable explanation for the highly vascularized and proliferative nature of parapoxvirus lesions. Disruption of this VEGF-like gene in ORFV causes a marked reduction in the vascularization and, surprisingly, epidermal proliferation and scab formation (55, 76). VEGF proteins from ORFV have been demonstrated to be mitogenic for endothelial cells and capable of inducing vascular permeability (44, 55). In the past, the viral VEGFs were thought to be different from the mammalian VEGF family in their receptor-binding profile by binding and cross-linking VEGFR-2 but not VEGFR-1 or VEGFR-3 (22, 27, 39, 69). However, a functionally distinct VEGF encoded by BPSV can bind both VEGFR-1 and VEGFR-2 (27).

Infectious spleen and kidney necrosis virus (ISKNV) is a member of the family *Iridoviridae*. Based on the eighth report of the International Committee on Taxonomy of Viruses, the family

* Corresponding author. Mailing address: State Key Laboratory for Biocontrol, School of Life Sciences, Sun Yat-sen (Zhongshan) University, 135 Xingang Road West, Guangzhou 510275, People's Republic of China. Phone: 86 20 84110976. Fax: 86 20 84113819. E-mail: Lsshjg@mail.sysu.edu.cn.

† These authors contributed equally to this work.

▽ Published ahead of print on 27 February 2008.

TABLE 1. Primers for real-time PCR

Gene	Sequence	
	Sense	Antisense
β-Actin	5′-ATG CCC CTC GTG CTG TTT TC-3′	5′-GCC TCA TCT CCC ACA TAG GA-3′
tie1	5′-AGC CCA GAA ACT GTG ATG ATG-3′	5′-GTT GAC AT AAG CCT TCC GTG C-3′
flk1	5′-GAT GGA GAT ACA CAC CTT CAG-3′	5′-TGC GTA CCG ATG ACA CAT TTC-3′
scl	5′-ACA GTG GTT TTG CTG GAG ATG-3′	5′-GTT CTT GCT GAG TTT CTT GTC-3′
gata1	5′-GTC CAG TTC GCC AAG TTT AC-3′	5′-GGG TTG TAG GGA GAG TTT AG-3′

Iridoviridae has been subdivided into five genera, including *Iridovirus*, *Chloriridovirus*, *Ranavirus*, *Lymphocystisvirus*, and *Megalocytivirus* (6). Iridoviruses are icosahedral cytoplasmic DNA viruses that infect invertebrates and poikilothermic vertebrates, including insects, fish, amphibians, and reptiles (64, 73). The viral genomes are both circularly permuted and terminally redundant, which are unique features of eukaryotic virus genomes (10, 11, 12, 65). Additionally, the iridoviruses that infect vertebrates have highly methylated genomes (10, 74).

In recent years, megalocytiviruses have attracted more attention because of their ecological and economic impact on wild and cultured fishes. ISKNV, Red Sea bream iridovirus, and closely related isolates infect a wide range of both marine and freshwater fish species including mandarin fish, *Siniperca chuatsi* (24); Red Sea bream, *Pagrus major* (28); sea bass, *Lateolabrax* sp. (29); brown-spot grouper, *Epinephelus tauvina* (8); rock bream, *Oplegnathus fasciatus* (30); African lampeye, *Aplocheilichthys normani* (63); large yellow croaker, *Larimichthys crocea* (5); orange-spotted grouper, *Epinephelus coioides* (38); Malabar grouper, *Epinephelus malabaricus* (9); angelfish, *Pterophyllum scalare* (53); grouper, *Epinephelus* sp. (7); tilapia, *Oreochromis niloticus* (41); dwarf gourami, *Colisa lalia* (63); red drum; and turbot, *Scophthalmus maximus* (59).

ISKNV is the type species of the genus *Megalocytivirus* and the causative agent of a disease with high mortality rates in mandarin fish and causing severe damage to mandarin fish cultures in China. Besides mandarin fish, ISKNV can infect large-mouth bass, *Micropterus salmoides*; zebrafish, *Ctenopharyngodon idellus*; and more than 50 species of marine fish (70). The prominent external features of ISKNV infection are petechial hemorrhages in the gill cover, lower jaw, eye, base of dorsal and ventral fins, caudal fin, and abdomen (25). The analysis of DNA sequences of ISKNV and other megalocytiviruses showed that they contained a domain similar to that of the platelet-derived growth factor/VEGF family, such as ISKNV ORF48R (24). However, the VEGF-like genes have not been found in the other four members of the family *Iridoviridae*, indicating that these viral VEGFs are unique to the megalocytiviruses (15).

Zebrafish as a model system has a number of advantages compared to mice, including rapid embryonic development and the ability to examine and manipulate embryos outside the animal (2, 3), and zebrafish is also a natural host of ISKNV. So, in this study, we used zebrafish as a model to demonstrate that ISKNV ORF48R is a new viral VEGF, first identified in fish viruses, which can induce vascular permeability and overexpression of *flk1* similarly to zebrafish $VEGF_{121}$.

MATERIALS AND METHODS

Zebrafish maintenance. Zebrafish embryos were maintained in Holt buffer on a 14-h-light/10-h-dark cycle at 28.5°C. The Holt buffer is composed of 3.5 g/liter NaCl, 0.2 g/liter $NaHCO_3$, 0.1 g/liter $CaCl_2$, and 0.05 g/liter KCl (pH 7.5). The stage of embryos was defined as hours postfertilization (hpf) or days postfertilization (dpf) (32).

Collection of ISKNV-infected fish. Moribund mandarin fish, *Siniperca chuatsi* (Basilewsky), from fish farms in Nanhai, Guangdong Province, China, which showed symptoms of ISKNV infection, were collected and kept at −80°C. Samples were examined by gross anatomy, PCR, and light and electron microscopy to confirm the disease as described previously (14, 71).

Virus and viral DNA. Virus was purified and DNA extraction was performed as described by Deng et al. (13). Spleen and kidney were removed from moribund mandarin fish and pulverized with a mortar and pestle in liquid nitrogen. The powdered tissue was gradually added to 10 volumes of phosphate-buffered saline (PBS; pH 7.4) and centrifuged at 5,000 × *g* for 20 min at 4°C. The supernatant was centrifuged at 35,000 × *g* for 30 min at 4°C. The resuspended pellet was layered on a 20 to 50% (wt/wt) sucrose gradient and further purified by centrifugation for 2 h at 90,000 × *g* in a SW40 Ti rotor (Beckman). The viral band in the gradient was removed, diluted threefold with PBS buffer, and centrifuged for 30 min at 90,000 × *g* at 4°C. The final pellet containing the nucleocapsid was resuspended in PBS buffer and incubated with 0.5% sodium dodecyl sulfate and 0.5 mg/ml proteinase K at 55°C for 3 h. The suspension was extracted using phenol-chloroform, and the DNA was precipitated with ethanol.

Sequence analysis. Amino acid sequences of VEGF from ISKNV (GenBank accession no. 19881405), large yellow croaker iridovirus (LYCIV) (GenBank accession no. 113200500), orange-spotted grouper iridovirus (OSGIV) (GenBank accession no. 62421189), rock bream iridovirus (RBIV) (GenBank accession no. 50237482), ORFV (GenBank accession no. 41018752), PCPV (GenBank accession no. 27464849), BPSV (GenBank accession no. 40019124), PVNZ (GenBank accession no. 115392307), human (GenBank accession no. 3719220), mouse (GenBank accession no. 38181775), sheep (GenBank accession no. 3228692), cattle (GenBank accession no. 163006), zebrafish (GenBank accession no. 3088576), medaka (GenBank accession no. 146760598), and rainbow trout (GenBank accession no. 49292179) were used for sequence analysis. Multiple sequence alignments were generated using ClustalW with default settings (http://www.ebi.ac.uk/clustalw). The phylogenetic tree was constructed using the Bootstrap N-J method of Phylip 3.63 programs. Trees were output using the program Treeview 1.6.6 (50). One thousand bootstrap analyses were performed for the phylogenetic tree.

Plasmid construction and microinjection. Based on the DNA sequence of ORF048R of ISKNV, a pair of primers were designed using Primer Premier 5.0 software as follows: 5′-CGG GAT CCA TGA GGT GCA CAG TGT TAC-3′ (sense), which contains a BamHI site, and 5′-CGG AAT TCC CGG CGC CGT GGT CCT C-3′ (antisense), which contains an EcoRI site. The fragments amplified by PCR from ISKNV genomic DNA were digested with BamHI and EcoRI (New England Biolabs) and then cloned into the pcXGFP vector. This plasmid was designated pG48R.

The total RNA of adult zebrafish was extracted with the SV Total RNA Isolation kit (Promega), and the cDNA was synthesized by Moloney murine leukemia virus (Promega). Sequences encoding $VEGF_{121}$ and other isoforms were amplified by PCR using the sense primer 5′-CGG GATC CATG AAC TTG GTT GTT TAT TTG-3′, which contains a KpnI site, and the antisense primer 5′-CGG AAT TCT CTT GGC TTT TCA CAT C-3′, which contains an EcoRI site. The PCR products were digested with KpnI (New England Biolabs) and EcoRI and then cloned into the pcXGFP vector. This plasmid was designated pGV121. The sequences of pG48R and pGV121 were confirmed by sequencing (Invitrogen).

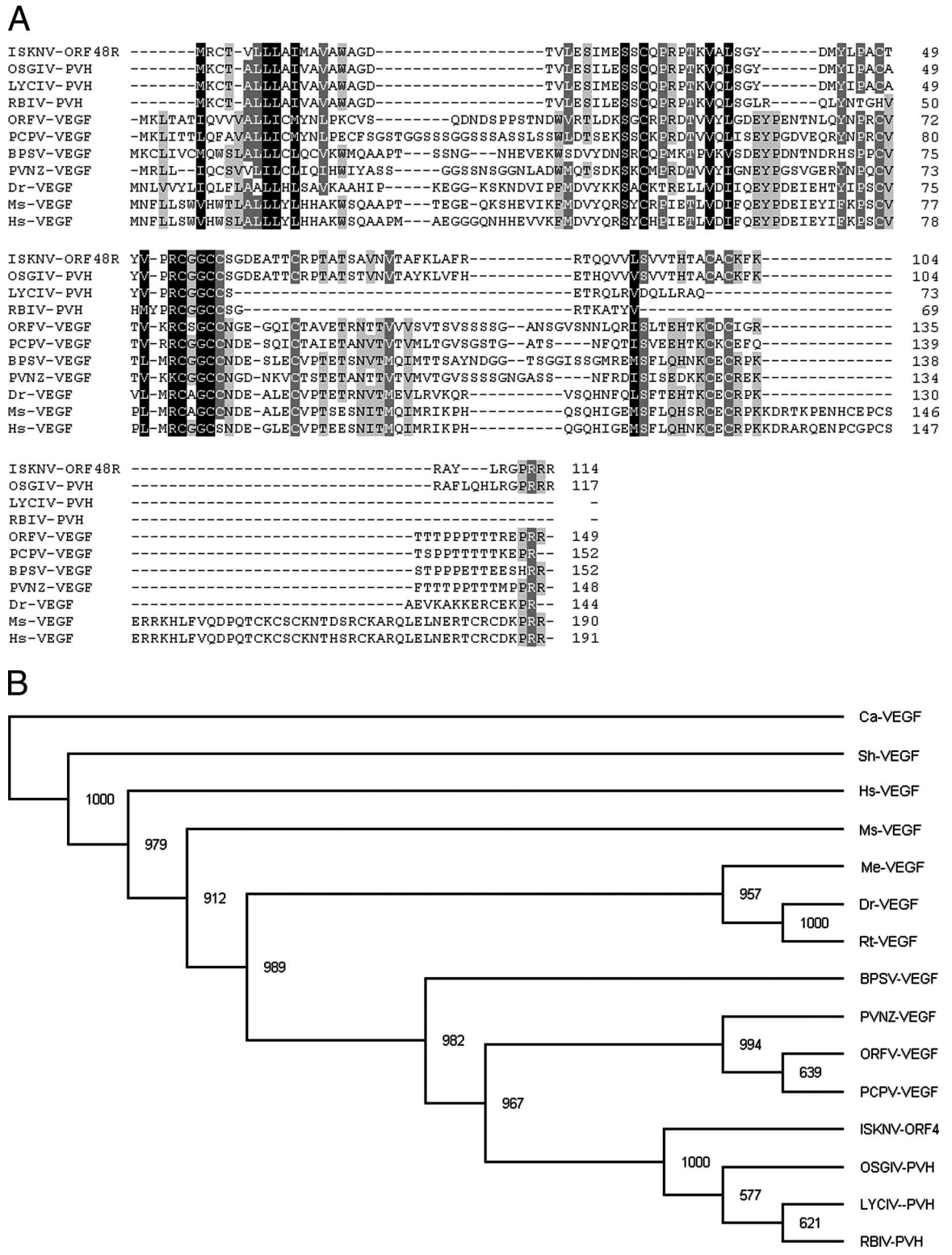

FIG. 1. Sequence feature of ISKNV ORF48R. (A) Alignment of the VEGF homologues of human, rat, zebrafish, ISKNV, RBIV, OSGIV, LYCIV, ORFV, PCPV, BPSV, and PVNZ. Black shading indicates 100% identity, medium-gray shading shows 80% to 100% identity, and light-gray shading shows 60% to 80% identities. (B) Phylogenetic tree of VEGF-like sequences. The diverse VEGF sequences were analyzed using the ClustalW program. The phylogenetic tree was constructed using the Bootstrap N-J method of Phylip 3.63 programs, and the tree was output using the program TreeView 1.6.6 (50). The bootstrap test of phylogeny was calculated with 1,000 replicates. Abbreviations: Hs, *Homo sapiens*; Ms, *Mus musculus*; Dr, *Danio rerio*; Sh, sheep; Ca, cattle; Me, Medaka; Rt, rainbow trout; PVH, predicted VEGF homologues.

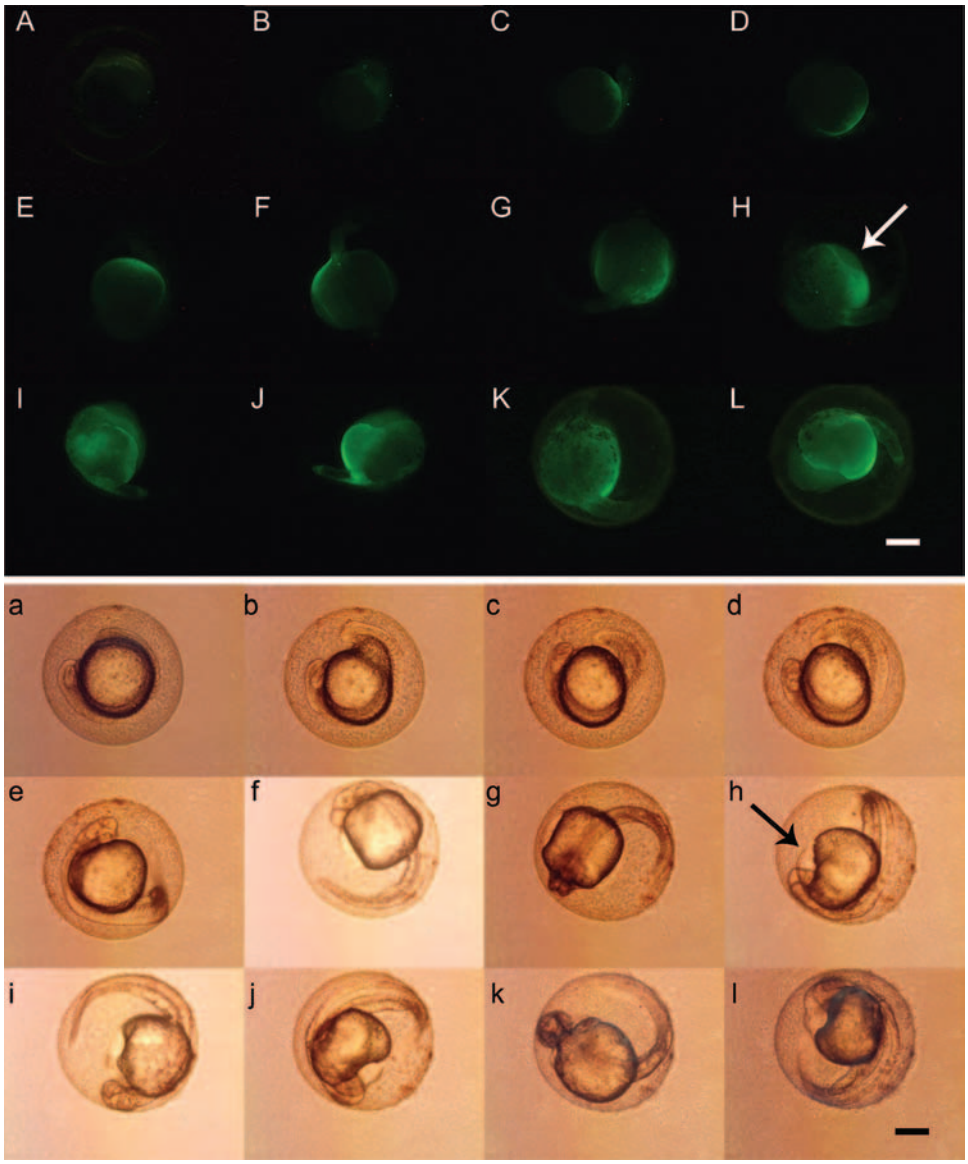

FIG. 2. Morphological changes induced by pG48R during zebrafish early embryonic development. The expression profile of pG48R is shown at the following stages: 14 (A and a), 16 (B and b), 18 (C and c), 20 (D and d), 22 (E and e), 24 (F and f), 26 (G and g), 28 (H and h), 30 (I and i), 32 (J and j), 34 (K and k) hpf, and 36 (L and l). Fluorescence (upper panels) and normal (lower panels) images of zebrafish embryos expressing the fusion gene were recorded continuously for 20 h after embryonic injection. The white arrow in panel H and the black arrow in panel h indicate the position of the dilated endocardium in the injected embryos. Embryos shown in panels F, f, G, g, H, I, K, k, and L are dorsal views. All others are lateral views. Bar, 250 μm for all panels.

Plasmids were linearized with BglII, purified with the QIAquick PCR purification kit (Qiagen), and then resuspended in water at a concentration of 150 ng/μl. The linearized plasmid DNA, pcXGFP, pG48R, pGV121, or pG48R plus pGV121, was injected into zebrafish wild-type embryos at the one-cell stage, and the volume of injection was about 1 to 2 nl per embryo. The wild-type and pcXGFP-injected embryos were used as negative controls.

Zebrafish embryos were visualized with a Leica MZFLIII stereomicroscope and photographed using a Leica DFC300 digital camera.

Single-embryo time-lapse microscopy. To study the dynamic changes of the VEGF-like gene and the developmental status of zebrafish, fluorescence images of zebrafish embryos expressing the fusion gene were recorded continuously for 20 h after embryonic injection. Embryos expressing the fusion gene were selected and incubated on a 25-mm-diameter round coverslip, which was placed in a thermally regulated chamber (INU-F1 microscopic incubation system; Tokai Hit, Shizuoka, Japan) mounted on the stage of a Nikon TE-2000S inverted microscope (Nikon, Melville, NY). The incubation temperature was maintained at 29°C. The fluorescence images and normal images were recorded using a cooled charge-coupled device camera, and the recording intervals were 30 min.

Real-time PCR. At 24 h, 48 h, 72 h, 4 days, and 5 days post-injection of pG48R, total embryonic RNA was isolated from zebrafish embryos using the SV Total RNA Isolation kit (Promega, Madison, WI) in accordance with the manufacturer's instructions. All RNAs were then reverse transcribed into cDNAs that were suitable for real-time PCR analysis using the ExScript RT-PCR kit (TaKaRa, Japan). To synthesize cDNA, 0.5 mM deoxynucleoside triphosphate, 50 pmol random hexamers, 50 U ExScript reverse transcriptase (200 U/μl), 10 U RNase inhibitor, 500 ng total RNA, and 1× reaction buffer were mixed in each reaction tube (10 μl per reaction) and then incubated at 42°C for 15 min, followed by a 2-min incubation at 95°C to inactivate the ExScript reverse transcriptase. Oligonucleotide primers for β-actin, *tie1*, *flk1*, *scl*, and *gata1* are \chatn shown in Table 1. All amplifications and detections were carried out in the Applied Biosystems

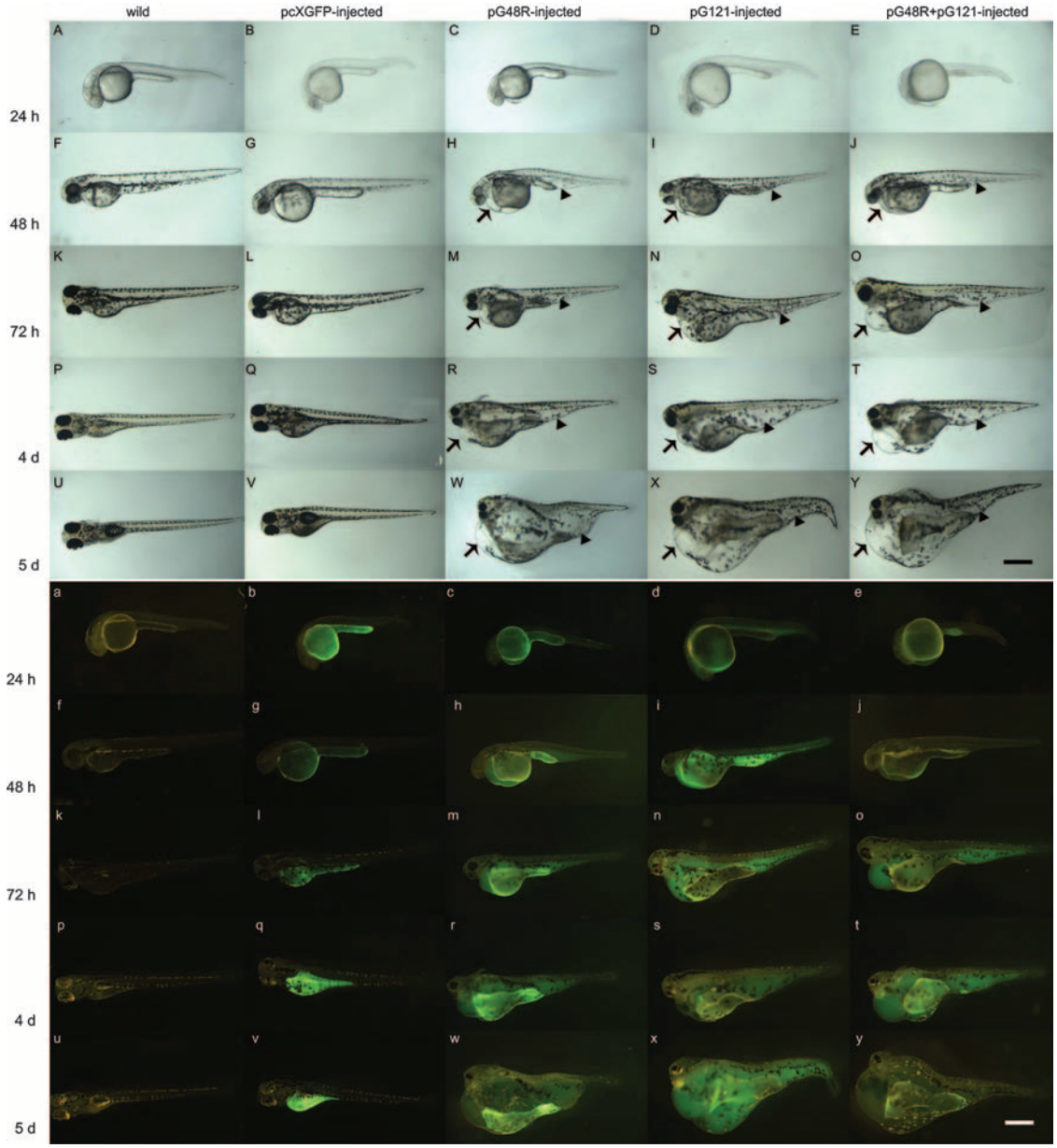

FIG. 3. Aberrant phenotypes induced by pG48R, pGV121, and pG48R plus pGV121 in the zebrafish embryonic development. Embryos were injected with linearized pcXGFP, pG48R, pGV121, and pG48R plus pGV121, 0.15 to 0.2 ng each, and then observed at 24 hpf (A to E and a to e), 48 hpf (F to K and f to k), 72 hpf (L to P and l to p), 4 dpf (Q to U and q to u), and 5 dpf (V to Y and v to y). White light (upper panels) and fluorescence (lower panels) images of zebrafish embryos expressing pcXGFP (b, g, l, q, and v), pG48R (c, h, m, r, and w), pGV121 (d, i, n, s, and x), and pG48R plus pGV121 (e, j, o, t, and y) were recorded continuously for 5 days after embryonic injection in zebrafish. In panels H, I, J, M, N, O, R, S, T, W, X, and Y, arrows indicate the dilating endocardium and arrowheads indicate the dilation in the tail region. All embryos are shown as lateral views with anterior to the left. Bar, 500 μm for all panels.

Prism 7000 system (Applied Biosystems, Foster City, CA) using the ExScript Sybr green QPCR kit (TaKaRa) and the following program: 95°C for 10 s, one cycle, and 95°C for 5 s and 62°C for 31 s, 40 cycles, followed by a 30-min melting curve collection, which was used to verify the primer dimers. Statistical analyses were performed using the $2^{-}3^{\Delta\Delta CT}$ relative quantification method.

RNA in situ hybridization. For whole-mount RNA in situ hybridization, zebrafish embryos injected with the linearized plasmid pcXGFP, pG48R, pGV121, or pG48R plus pGV121 were fixed in 4% paraformaldehyde overnight at 4°C. For embryos older than 24 hpf, they were first incubated in 0.003% 1-phenyl-2-thiourea to remove pigments before fixation (35, 36).

cDNA sequences of *flk1* were PCR amplified and cloned into pGEM-T Easy vector (Promega) as templates to generate an antisense riboprobe for in situ hybridization. The following primers were used: 5′-AGG ACC CAG ACT ATG TCC GCA AAG-3′ (sense) and 5′-TCT TCA TCG CTC GGG ACA TG-3′ (antisense) for *flk1*. Whole-mount in situ hybridization was performed using digoxigenin-labeled RNA probes essentially as described previously (23, 56). The wild-type and pcXGFP-injected embryos were used as negative controls.

Immunoprecipitation. A DNA sequence corresponding to the sequence encoding amino acid residues 1 to 736 covering the full outer membrane region of the zebrafish *flk1* gene was PCR amplified from embryo cDNA of zebrafish using forward primer *Flk-F* (5′-CACCGAGCTCCACCATGACTCCTCTTAAAACC TC-3′) together with the reverse primer *Flk-R* (5′-TCCCCGCGGTTGGTTTA CCATCTTCTCCTAC-3′) and cloned in frame into the pEGFP-N3 vector (Clontech) to generate PN-flk vector to express a green fluorescent protein

(GFP) fusion protein. The full-length sequence of ISKNV ORF48R was cloned into the pcDNA3.1 V5/His vector to generate PC-48V5 vector, expressing a V5-tagged VP48R protein.

PC-48V5 was cotransfected with PN-flk into fathead minnow (FHM) fish cells, and 72 h later the cells were collected and lysed. Immunoprecipitation was performed using anti-V5 antibody (Invitrogen) and detected by Western blotting using the rabbit anti-GFP antibody (Sigma). PC-48V5/pEGFP-N3-cotransfected FHM cells were used as a control.

PC-flkV5 vector, expressing a V5-tagged FLK protein, and PN-48 vector, expressing a GFP-tagged ISKNV 048R protein, were constructed as the control of reciprocal precipitations and cotransfected into FHM cells. Immunoprecipitations were performed with the collected cells by using anti-V5 antibody and detected by Western blotting using the rabbit anti-GFP antibody.

Knockdown of FLK-1 expression with antisense morpholino-oligonucleotides. The antisense morpholino-oligonucleotide (Mo) of *flk1* was obtained from Gene Tools, LLC. The sequence of anti-*flk1* Mo was 5′-CCGAATGATACTCCGTA TGTCAC-3′ (54). Inert standard Mos, which have no effect on zebrafish development, were used as negative controls. The negative-control Mo (NC-Mo) (0.25 mM, 5′-CCTCTTACCTCAGTTACAATTTATA-3′), tagged with fluorescein at the 3′ end (33), was mixed into samples to monitor the success of injection and distribution of the respective Mos in the embryos. Lyophilized powder was resuspended in water at the concentration of 3 mM. Then the *flk1* Mo solution, mixed with the linearized plasmid pG48R with the working concentration of 150 ng/μl, was diluted to a working concentration of 1.5 mM, prior to injection into one-cell embryos. The volume of injection was about 1 to 2 nl per embryo.

Mo-injected zebrafish embryos were visualized with an Olympus SZX16 stereomicroscope and photographed using an Olympus DP71 digital camera.

RESULTS

Cloning and sequence analysis of ISKNV ORF048R. As a first step to investigate the biological function of ISKNV ORF048R, we amplified, purified, cloned, and sequenced ISKNV ORF048R DNA fragments and found that ORF48R is 345 bp long, encoding 114 amino acids (Fig. 1A). Analysis of the amino acid sequence of ORF48R with the SMART program showed that ORF48R contains a domain (residues 27 to 103) similar to that of the platelet-derived growth factor and VEGF families. To compare the features of the ISKNV ORF048R sequence with those of VEGF isoforms found in LYCIV, OSGIV, RBIV, ORFV, PCPV, BPSV, PVNZ, human, mouse, and zebrafish, we aligned them using the ClustalW program. Multiple sequence alignment revealed that ISKNV ORF048R shares a central VEGF homology domain with the members of the VEGF family and has a relatively high similarity to other VEGF isoforms (Fig. 1A). ISKNV ORF048R protein shows higher similarity with VEGF members from *Megalocytivirus* than with those from other species, and it is 49.2% identical to LYCIV VEGF (GenBank accession no. 113200500), 90.6% identical to OSGIV VEGF (GenBank accession no. 62421189), and 46.6% identical to RBIV VEGF (GenBank accession no. 50237482). ISKNV ORF048R protein also shows higher similarity to homologues found in members of the *Parapoxvirus* genus than to those in fish and mammals, and it is 38.4% identical to ORFV VEGF (GenBank accession no. 41018752), 38.7% identical to PCPV VEGF (GenBank accession no. 27464849), 33.1% identical to BPSV VEGF (GenBank accession no. 40019124), and 38.1% identical to PVNZ VEGF (GenBank accession no. 115392307). The ISKNV ORF048R protein shows relatively low similarity with its mammalian homologues and is 29.2% identical to human VEGF (GenBank accession no. 3719220) and 32.5% identical to mouse VEGF (GenBank accession no. 38181775) but 39.7% identical to zebrafish VEGF (GenBank accession no. 3088576).

TABLE 2. Percentages of embryos with abnormal phenotypes among the surviving injected embryos[a]

Injected material and expt no	No. of embryos			% of embryos with abnormal phenotype	
	Injected	With fluorescence	With abnormal phenotype	In each expt	Avg ± SD for group
pcXGFP					0
1	199	121	0	0	
2	189	107	0	0	
3	167	98	0	0	
pG48R					53.58 ± 0.89
1	59	32	32	54.2	
2	89	48	48	53.9	
3	78	41	41	52.6	
pGV121					45.53 ± 1.93
1	194	84	84	43.3	
2	146	68	68	46.6	
3	152	71	71	46.7	
pG48R plus pGV121					74.70 ± 1.82
1	98	72	72	73.5	
2	112	86	86	76.8	
3	107	79	79	73.8	

[a] The embryos were at the stage of 48 hpf. The data shown here were collected from three individual injection experiments. The embryos were injected at the one-cell stage. Approximately 0.15 to 0.2 ng of pcXGFP, pG48R, pGV121, and pG48R plus pGV121 was injected in each embryo.

To further explore the evolutionary origin of VEGF isoforms, we searched for diverse VEGF-like sequences in the NCBI and Ensembl databases and performed a phylogenetic analysis (Fig. 1B). In this analysis, we chose representative VEGF-like sequences from four members of the *Megalocytivirus* genus (ISKNV, LYCIV, OSGIV, and RBIV), four members of the *Parapoxvirus* genus (ORFV, PCPV, BPSV, and PVNZ), zebrafish, medaka, rainbow trout, human, mouse, sheep, and cattle. The result shows that the ISKNV ORF48R and VEGF homologues from LYCIV, OSGIV, and RBIV are placed in a monophyletic group and this group is evolutionarily closest to members of the *Parapoxvirus* genus (ORFV, PCPV, BPSV, and PVNZ). The viral VEGFs from *Megalocytivirus* and *Parapoxvirus* are evolutionarily more closely related to those from zebrafish, medaka, and rainbow trout and relatively distant from VEGFs of mammals, such as human, mouse, sheep, and cattle.

Overexpression of pG48R resulted in the abnormal embryo phenotype during zebrafish embryogenesis. We cloned the cDNA fragment of ISKNV ORF048R into the vector pcXGFP to construct recombinant plasmid pG48R. This plasmid was used to test the influence of ORF048R overexpression on zebrafish embryonic development.

After pG48R was injected into one-cell-stage zebrafish embryos, we found that expression of pG48R began at 13 to 14 hpf (Fig. 2A), and it was located in a region adjacent to the yolk throughout the embryo, especially in the prospective heart fields. Subsequently, the expression became more and more enhanced, and at 28 to 30 hpf the whole yolk sac was full of fluorescence (Fig. 2H). At the same time a noticeable enlargement of the pericardium was observable (Fig. 2h)

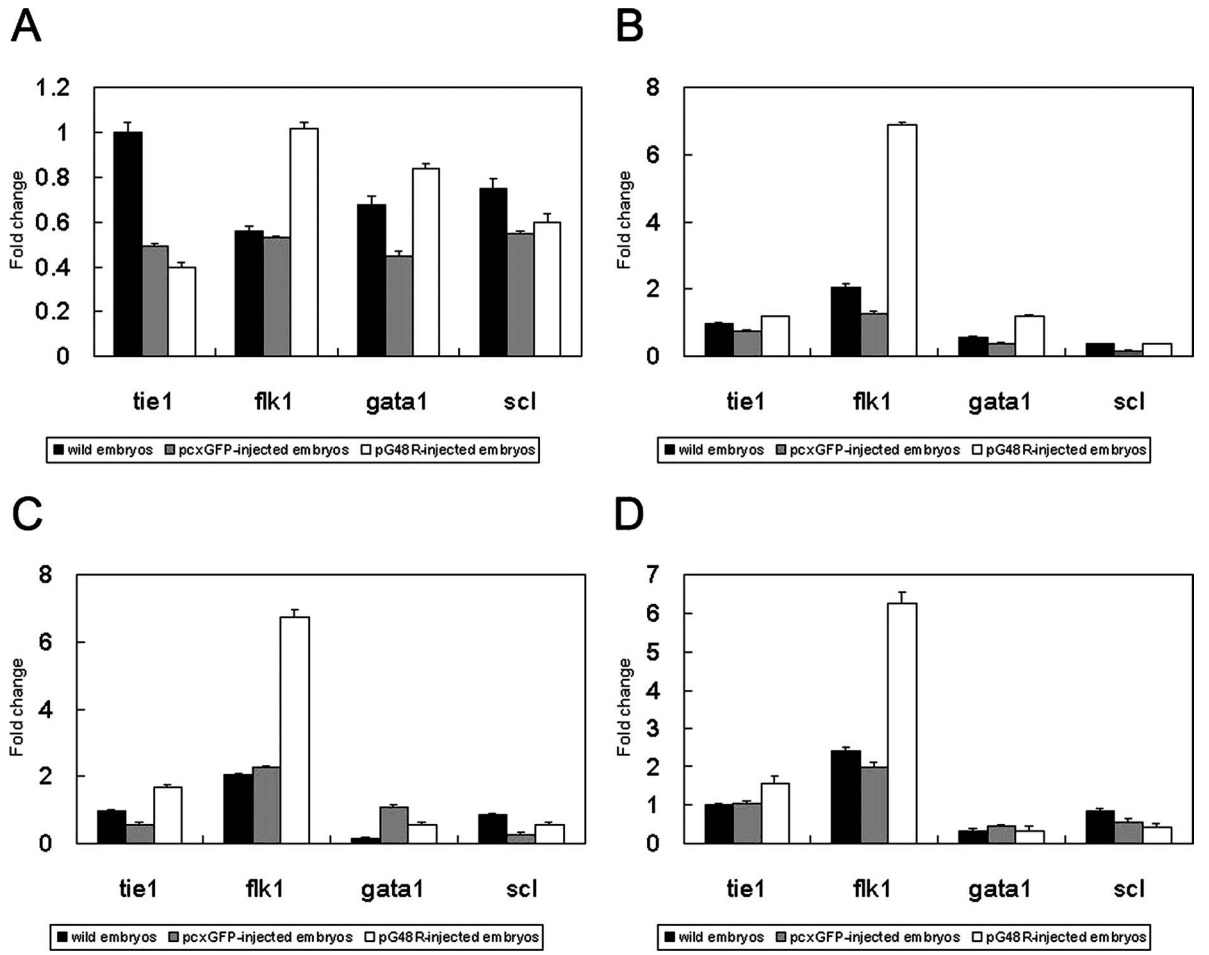

FIG. 4. Quantitative PCR analysis of the expression of vascular endothelial and hematopoietic cell marker genes induced by pG48R in the zebrafish embryonic development. Expression of *tie1*, *flk1*, *gata1*, and *scl* at the zebrafish developmental stages at 24 hpf (A), 48 hpf (B), 72 hpf (C), and 4 dpf (D). The black column represents the average expression value of the marker genes in wild-type embryos. The gray column represents the average expression value of the marker genes in pcXGFP-injected embryos. The white column represents the average expression of the marker genes in pG48R-injected embryos. The expression level of β-actin was set as 1. Results of relative quantification were analyzed with the method of Liu and Saint (37).

compared to the wild-type embryos and the pcXGFP-injected embryos. After 48 hpf, in addition to the evidently dilated pericardiac edema (Fig. 3H, M, R, and W), dilation also appeared in the ventral tail region (Fig. 3H, M, R, and W), which also has fluorescence (Fig. 3h, m, r, and w). At 4 to 5 dpf, the whole ventral embryonic body became a huge vacuole (Fig. 3R and W), the yolk sac mostly disappeared, and the zebrafish larvae did not swim actively. After 5 dpf, the zebrafish larvae began to die in succession, and after about 10 to 14 days all abnormal larvae died. Statistically, the percentage of embryos that have an abnormal phenotype was 53.6% (the average value of three individual injection experiments) in the pG48R-injected embryos (Table 2), which showed that the abnormal phenotype was induced by pG48R and not physical trauma.

The abnormal phenotype induced by pG48R is similar to that induced by pGV121 during zebrafish embryogenesis. Based on the above sequence and structural analysis of ORF48R and zebrafish VEGF, we found that ORF48R may be structurally and functionally related to zebrafish $vegf_{121}$ (75). In order to test whether ORF48R has functions similar to zebrafish $vegf_{121}$, we also cloned zebrafish $vegf_{121}$ into the vector pcXGFP to generate pGV121 and microinjected pGV121 into one-cell-stage zebrafish embryos in the same way as pG48R. Through the observation of the embryonic development of the pGV121-injected embryos from 24 hpf to 5 dpf (Fig. 3D, I, N, S, and X), we found that the abnormal phenotypes induced by overexpression of pGV121 were highly similar to those induced by pG48R, including obvious pericardial edema and dilation at the tail region, compared to the wild-type and pcXGFP-injected embryos. At 5 dpf, the morphological characteristics induced by pG48R and pGV121 were almost identical (Fig. 3W and X). Moreover, pG48R and pGV121 were expressed in the same position during zebrafish embryonic development (Fig. 3c, h, m, r, w, d, i, n, s, and x). Statistically, the percentage of embryos that showed an abnormal phenotype was 45.5% (the average value of three individual injection experiments) in the pGV121-injected embryos (Table 1), close to that of pG48R-injected embryos. These results suggest that ISKNV

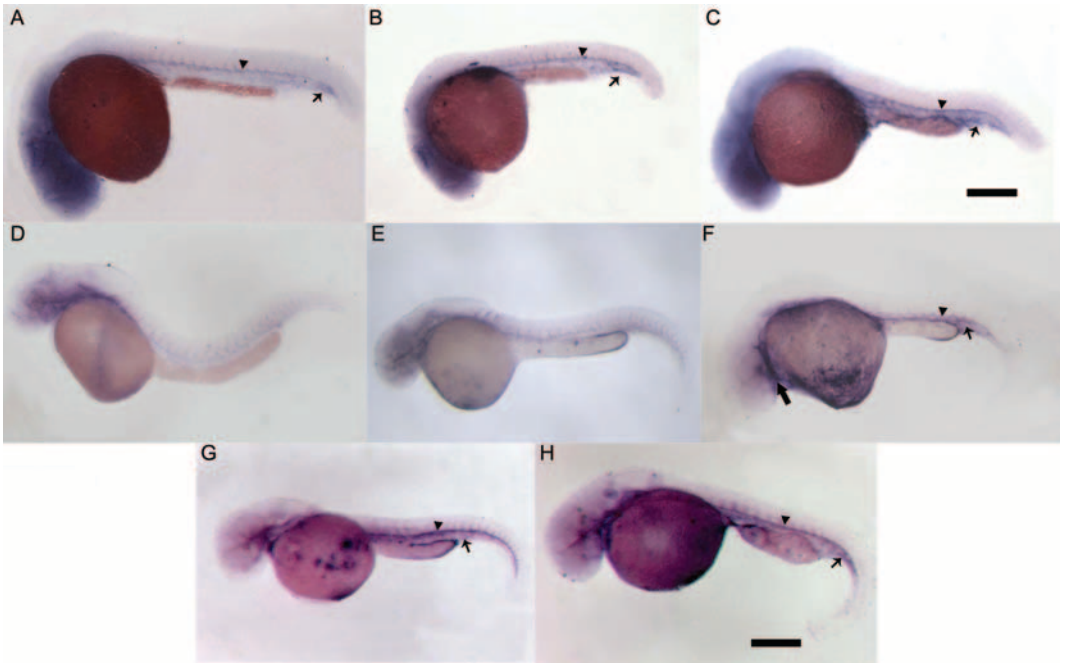

FIG. 5. RNA in situ hybridization of *flk1* expression induced by pG48R during early embryogenesis. Embryos shown in panels A to C were at 24 hpf. Embryos shown in panels D to H were at 48 hpf. At 24 hpf, compared to the wild-type embryos (A) and pcXGFP-injected embryos (B), the *flk1* expression in pG48R-injected embryos (C) was enhanced in the dorsal aorta (A to C, arrowhead) and the tail region (A to C, arrow). At 48 hpf, the position and up-regulated expression of *flk1* (F, arrowhead and arrow) in pG48R-injected embryos were similar to those in pGV121-injected embryos (G, arrowhead and arrow) and pG48R-pGV121-coinjected embryos (H, arrowhead and arrow), compared to the wild-type embryos (D) and pcXGFP-injected embryos (E). In addition, the up-regulated expression of *flk1* in the endocardium was also observed (F, large arrow). Embryos shown in all panels are lateral views with anterior to the left. Bars, 300 μm (A to C) and 500 μm (D, E, F, G, and H).

ORF048R has high functional similarity to zebrafish $VEGF_{121}$.

The cooperative effect exists between ISKNV ORF048R and zebrafish $VEGF_{121}$. It is well known that the cooperative effect of *vegf* isoforms is stronger than that of a single *vegf* isoform (34). In order to test whether $VEGF_{121}$ and ISKNV ORF048R have a cooperative effect, we coinjected pGV121 plus pG48R (1:1) into one-cell-stage zebrafish embryos. Phenotypic observation of the embryos coinjected with pG48R plus pGV121 at 72 hpf, 4 dpf, and 5 dpf showed that the dilated pericardiac edema induced by pGV121 and pG48R together (Fig. 3 O, T, and Y) was obviously more severe than that of pGV121-injected or pG48R-injected embryos. Statistically, the percentage of embryos that had an abnormal phenotype was 74.7% (the average value of three individual injection experiments) in the coinjected embryos (Table 1), higher than that of pG48R- (53.6%) or pGV121-injected embryos (45.5%) (Table 1). Together, these results suggest that ISKNV ORF048R and $VEGF_{121}$ could cooperate with each other to enhance the induced effect.

FLK-1 plays an important role in ISKNV ORF048R-induced abnormal phenotypes of zebrafish embryos. We assayed for the influence of pG48R overexpression on expression of hematopoietic cell marker genes, *scl* and *gata1*, and vascular endothelial cell-specific marker genes, *flk1* and *tie1*, using real-time PCR. The results showed that at 24 hpf the expression of the marker gene *flk1* in pG48R-injected embryos was up-regulated about one- to twofold compared to the wild-type embryos or pcXGFP-injected embryos (Fig. 4A). At 48 hpf, 72 hpf, and 4 dpf, the expression of *flk1* in pG48R-injected embryos was significantly up-regulated and enhanced about three- to fivefold compared with the wild-type embryos or pcXGFP-injected embryos (Fig. 4B, C, D, and E). Similar results were also observed at 5 dpf (data not shown). However, the expression levels of three other marker genes (*scl*, *gata1*, and *tie1*) were not obviously influenced by overexpression of ORF48R (Fig. 4A, B, C, D, and E). Therefore, we demonstrated that the endothelial cell-specific tyrosine kinase receptor FLK-1 is an important receptor for ORF048R to activate signal transduction pathway in zebrafish.

By performing the whole-mount in situ hybridization, we further confirmed that the influence of ISKNV ORF048R on *flk1* was at the level of transcription during zebrafish embryogenesis. At 24 and 48 hpf, expression of *flk1* was up-regulated (Fig. 5C and F) compared to the control embryos (Fig. 5A and B). *flk1* expression was highly increased in the entire vasculature of the embryo (Fig. 5F) compared to the control embryos (Fig. 5D and E). High levels of *flk1* were observed in the endocardium of the injected embryos (Fig. 5F). In the trunk, *flk1* expression was greatly up-regulated with higher transcription levels in the dorsal aorta and the axial vein. In some embryos, the entire area between the two major trunk vessels was full of *flk1*-positive cells (Fig. 5C). Up-regulation of *flk1* expression in pG48R- or pGV121-injected embryos was weaker than that in pG48R-plus-pGV121-coinjected embryos, further demonstrating that ORF048R could cooperate with zebrafish $VEGF_{121}$ to exert a stronger effect on the formation of new blood vessels during vasculogenesis and angiogenesis in zebrafish.

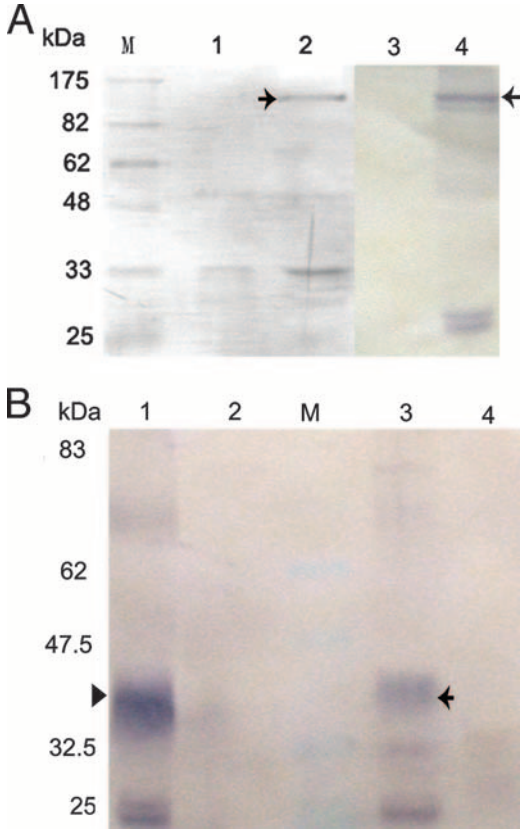

FIG. 6. Immunoprecipitation analysis of the interactions between VP48R and FLK-1. Lane M is molecular size markers. (A) The expression vector PC-48V5 together with the expression vector PN-flk or the empty pEGFP-N3 vector were used to cotransfect FHM cells. Cytoplasmic extracts from these cells were immunoprecipitated with an anti-V5 monoclonal antibody and detected by Western blotting using the anti-GFP antibody. (Lane 1) As a control, no band corresponding to the GFP (28K) was detected in the immunoprecipitation analysis by using cells cotransfected with PC-48V5 and pEGFP-N3 vectors. (Lane 2) FLK-GFP protein (black arrow) was coprecipitated by VP48R. (Lane 3) Lysates of FHM cells showed no positive signals to anti-GFP antibody. (Lane 4) Western blot analysis showed the band corresponding to the FLK-GFP protein in the lysates of FHM cells cotransfected with PN-flk and PC-48V5. (B) The expression vector PC-flkV5/PN-48 or PC-flkV5/pEGFP-N3 was used to cotransfect FHM cells. Cytoplasmic extracts from these cells were immunoprecipitated with an anti-V5 monoclonal antibody and detected by Western blotting using the anti-GFP antibody. (Lane 1) Lysates of FHM cells showed no positive signals to anti-GFP antibody. (Lane 2) Western blot analysis showed the band corresponding to the FLK-GFP protein in the lysates of FHM cells cotransfected with PN-48 and PC-flkV5. (Lane 3) The band corresponding to the 48-GFP protein (40.5K) (black arrowhead) was detected in the immunoprecipitation analysis by using FHM cells cotransfected with PC-flkV5 and PN-48 vectors. (Lane 4) As the control, no band corresponding to the GFP (28K) was detected in the immunoprecipitation analysis by using FHM cells cotransfected with PC-flkV5/pEGFP-N3.

Immunoprecipitation analysis of the interactions between ORF048R and FLK-1 showed that FLK-1–GFP was coprecipitated by ORF048R-V5 (black arrow in Fig. 6A, lane 2) compared to the control, in which no band corresponding to the GFP (28K) (lane 1 in Fig. 6A) was detected in the immunoprecipitation analysis using cells cotransfected with PC-48V5 and pEGFP-N3 vectors. The *flk* construct was confirmed to be adequately expressed in FHM cells cotransfected with PN-flk and PC-48V5 with Western blot analysis (black arrow in lane 4 in Fig. 6A), compared to the control of nonprecipitated lysates from FHM cells (lane 3 in Fig. 6A). The 048 construct was also confirmed to be adequately expressed in FHM cells cotransfected with PN-48 and PC-flkV5 with Western blot analysis (black arrowhead in lane 1 in Fig. 6B), compared to the control of nonprecipitated lysates from FHM cells (lane 2 in Fig. 6B). The result of reciprocal precipitations showed that ORF048R-GFP was coprecipitated by FLK-1–V5 (black arrow in lane 3 in Fig. 6B), compared to the control, in which no band corresponding to the GFP fusion protein was detected in the immunoprecipitation analysis using FHM cells cotransfected with PC-flkV5 and pEGFP-N3 vectors (lane 4 in Fig. 6B).

This result of immunoprecipitation analysis of the interactions between ORF048R and FLK-1 showed that FLK-1 is the ISKNV ORF048R receptor in zebrafish.

Knockdown of *flk1* blocks ISKNV ORF48R-induced signaling during zebrafish embryogenesis. We knocked down the expression of *flk1* in zebrafish and then tested the effect of ORF48R overexpression on zebrafish embryonic development. The *flk*-Mo had been proved effective by Rottbauer et al. (54). However, the demonstration of the effectiveness of the *flk*-Mo was not successful with Western blotting by us, maybe because of the low protein content of the material prepared from the zebrafish embryos.

The wild-type embryos, or embryos injected with the NC-Mo or the *flk1* antisense Mos mixed with NC-Mo, which was used to monitor the success of injection, were injected with pG48R at the one-cell stage. At 48 hpf and 72 hpf, we found that the ectopic phenotype, such as dilated pericardiac edema, did not appear in *flk1*-Mo- and pG48R-coinjected embryos (Fig. 7J and K), compared to the controls. But at 4 dpf, compared to the wild-type embryos and the embryos injected with NC-Mo and pG48R, pericardial edema appeared in the embryos coinjected with the *flk1*-Mo and pG48R (Fig. 7L) and subsequently became more serious over the next several days. Meanwhile, pericardial edema also appeared in the embryos injected with the *flk1*-Mo mixed with NC-Mo at 4 dpf (Fig. 7I) but was less serious than that of *flk1*-Mo- and pG48R-coinjected embryos. These results showed that the *flk1*-Mo might knock down the expression of *flk1* and that ISKNV ORF48R might not bind with the receptor FLK-1 before 72 hpf.

It has been confirmed that Mo-mediated gene knockdown is effective at 4 and 5 dpf (57, 62), depending on the targeted gene. After 72 hpf, the effect of knockdown of *flk1*-Mo was weakened because of the invalidation of *flk1*-Mo in zebrafish and because then ORF48R bound with FLK-1 and resulted in pericardial edema. The result that pericardial edema induced by *flk1*-Mo and pG48R coinjection was more serious than that induced by the *flk1*-Mo and NC-Mo coinjection showed that ORF48R was the main factor in causing pericardial edema in zebrafish embryos after 72 hpf.

DISCUSSION

In this study, we compared the influences of overexpression of ISKNV ORF48R and zebrafish $VEGF_{121}$ on the vascular response during early embryonic development in zebrafish. Zebrafish $vegf_{121}$ overexpression may generate defects in the

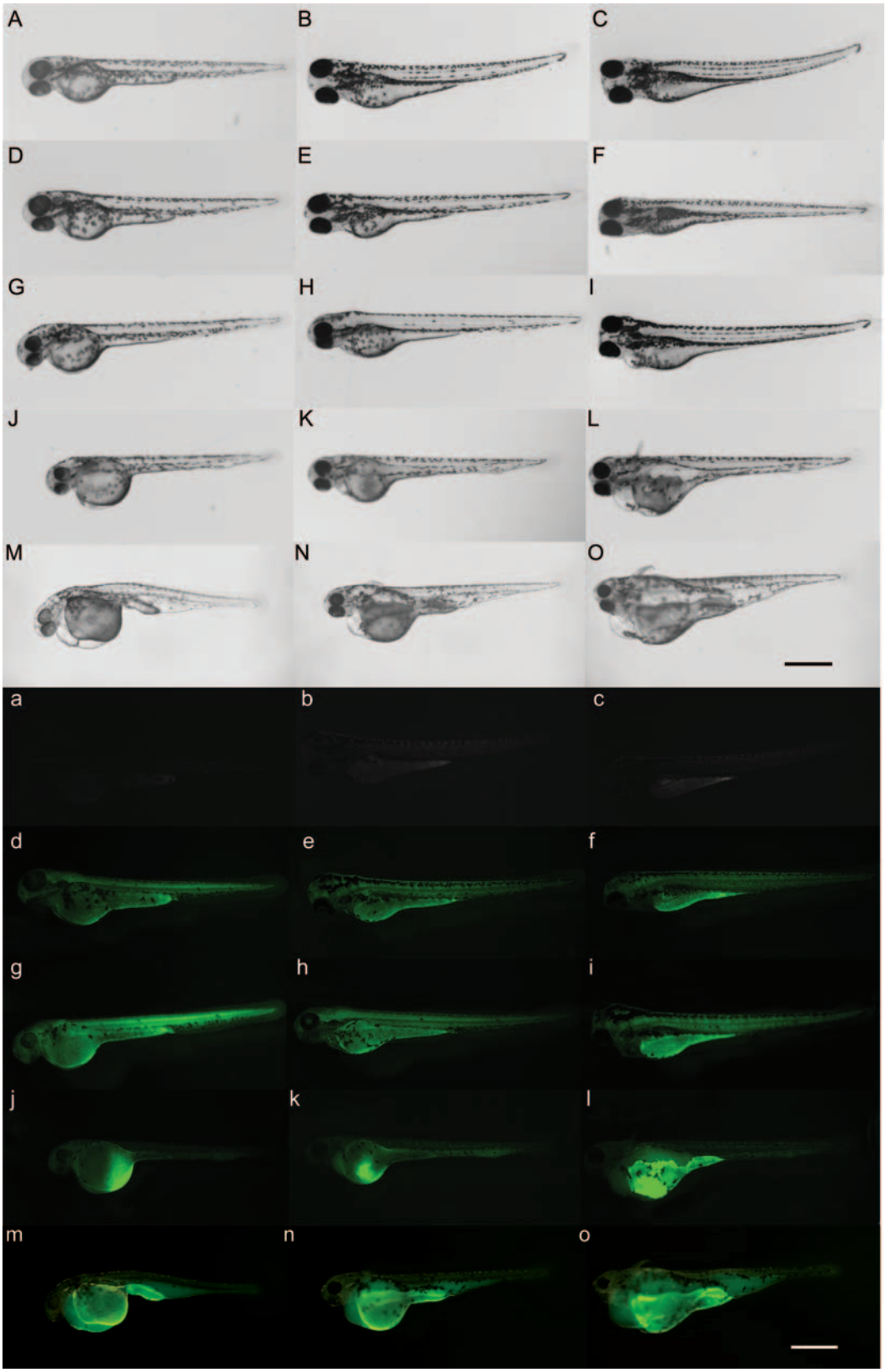

FIG. 7. Antisense knockdown of *flk1* in zebrafish abolishes ORF48R-induced effects. The wild-type embryos are shown in panels A and a (48 hpf), B and b (72 hpf), and C and c (4 dpf). The NC-Mo-injected embryos are shown in panels D and d (48 hpf), E and e (72 hpf), and F and f (4 dpf). The anti-*flk1*-Mo- and NC-Mo-coinjected embryos are shown in panels G and g (48 hpf), H and h (72 hpf), and I and i (4 dpf). The pG48R- and anti-*flk1*-Mo-coinjected embryos are shown in panels J and j (48 hpf), K and k (72 hpf), and L and l (4 dpf). The pG48R-injected embryos are shown in panels M and m (48 hpf), N and n (72 hpf), and O and o (4 dpf). Normal (upper panels) and fluorescence (lower panels) images of zebrafish embryos expressing the fusion gene were recorded continuously for 3 days after embryonic injection. Bar, 300 μm for all panels.

vasculature, which in turn results in pericardial edema and abnormal blood cell accumulation. For example, in the presence of excess VEGF, the reduced cardiac lumen due to endocardium hyperplasia may result in the obstruction of intracardiac blood flow, leading to pericardial fluid accumulation (34, 59). Our results show that overexpression of the ISKNV ORF48R gene also results in pericardial edema and abnormal blood cell accumulation in zebrafish (Fig. 1 and 5). In addition, the result from real-time PCR showed that ISKNV ORF48R can bind and up-regulate expression of FLK-1. Knockdown of *flk1* with antisense Mos blocked binding of ISKNV ORF48R to its receptor, although the effectiveness of *flk1*-Mo remains to be demonstrated; hence, pericardial edema and abdominal dilation were not observed before 72 hpf. However, we found that the embryos coinjected with the *flk1*-Mo and NC-Mo showed a normal phenotype before 72 hpf, but at 4 dpf, pericardial edema was also observed, although it was smaller than that of *flk1*-Mo- and pG48R-coinjected embryos. This result showed that knockdown of *flk1* with antisense Mos may cause pericardial edema to a certain extent after 72 hpf, whose mechanism might be similar to knockdown of *vegf* with antisense Mos (35). In zebrafish, FLK-1 has an essential role in vasculogenesis, angiogenesis, and hematopoiesis. FLK-1 can mediate VEGF-induced vascular dilation, proliferation of endothelial cells, and epidermal hyperplasia (20, 31, 47). FLK-1-deficient zebrafish embryos manifest more subtle effects on vessel formation (21). These results suggest that ISKNV ORF48R, like zebrafish $VEGF_{121}$, is a biologically active member of the VEGF family that interacts with the main mitogenic receptor, FLK-1. The interaction of ISKNV ORF48R with FLK-1 is likely to contribute to the proliferative and highly vascularized nature of the ISKNV lesion on its natural hosts, like mandarin fish. Recently, a duplicated zebrafish RTK locus termed Kdrb was isolated, which is homologous to FLK-1. Kdrb protein can cooperate with FLK-1 in mediating the vascular effects of VEGF-A in zebrafish (47). We speculate that ISKNV ORF48R may also interact with Kdrb, but the mechanism remains to be studied.

ISKNV ORF48R is highly related in its function to the VEGFs from ORFV and PCPV. The lesions resulting from the infection of zebrafish by ISKNV are similar to those of sheep, goat, or humans infected by ORFV and PCPV. The lesions of the zebrafish infected by ISKNV show vascular dilation and hemorrhages underlying the epidermis. The lesions resulting from infection by ORFV and PCPV include vascular dilation, dermal edema, and proliferation of endothelial cells, due to the presence of this VEGF homologue encoded by ORFV and PCPV (43, 55, 77). When the VEGF-like genes in ORFV and PCPV are disrupted, vascularization, epidermal proliferation, and scab formation are markedly reduced (27, 68). In our study, we did not inactivate the ISKNV VEGF gene but instead chose to knock down the viral VEGFR FLK-1. The results showed that the lesion induced by the ISKNV ORF48R was also not observed. Alternatively, the viral VEGFs encoded by parapoxvirus may bind and cross-link VEGFR-2. Our real-time PCR result also showed that the ISKNV ORF48R might up-regulate expression of *flk1* but not that of other receptors such as *tie1*, *scl*, and *gata1*. These results demonstrate that ISKNV ORF48R shares some of the functional features of zebrafish VEGFs but also shares many of those found in other viral VEGFs.

The roles played by the viral VEGF in the vascular response have been illuminated in ORFV lesions. If the viral VEGF gene is disrupted, the infection of ORFV's natural host would be significantly affected, although the growth of ORFV in cultured cells was not significantly influenced (52, 55). The viral VEGF can induce dermal vascularization and epidermal hyperplasia in ORFV lesions by changing the vascular permeability and releasing some growth factors, such as fibroblast growth factor 2, keratinocyte growth factor, and heparin-binding epidermal growth factor. Another possible role for the viral VEGF is helping scab formation and wound healing (55). The scab in the ORFV lesion can contain substantial amounts of infectious virus. The envelopment of the virus in the scab protects it from environmental inactivation. Although we do not know the roles that ISKNV ORF48R plays in ISKNV infection, we speculate that ISKNV ORF48R may play a vital role in the infection of its hosts and viral replication by inducing vascular proliferation and promoting permeability.

The evolutionary significance of the sequence and functional divergence between viral VEGFs and those from the fish and mammalian family remains to be investigated. Currently, there is some evidence suggesting that the VEGF encoded by BPSV may represent a more ancestral mammalian-like VEGF that has lost the ability to bind VEGFR-1 under lower selection pressure or may have resulted from a more recent and independent recombination event between a mammalian VEGF and BPSV (27). The result from our phylogenetic tree shows that viral VEGFs from *Megalocytivirus* are more closely related to their parapoxvirus homologues than to fish homologues. There may be two possibilities. The first one is that *Megalocytivirus* and *Parapoxvirus* may share the same ancestor, and the second one is that *Megalocytivirus* and *Parapoxvirus* may have different ancestors but their ancestors are closer in evolutionary relationship. On the other hand, the result from our phylogenetic tree also shows that virus-derived VEGFs are more closely related to fish VEGFs than mammalian VEGFs, suggesting that viral VEGFs may have evolved from fish VEGFs. However, parapoxvirus infects mammals but not fish, so it is unclear if the ancestral VEGFs of parapoxvirus have also evolved from fish VEGFs.

In conclusion, our studies demonstrated that a viral VEGF-like protein, ISKNV ORF48R, like zebrafish $VEGF_{121}$, functions as a potent growth factor to stimulate angiogenesis and can bind its receptor FLK-1 to affect zebrafish early embryonic vascular development.

ACKNOWLEDGMENTS

This research was supported by the National Natural Science Foundation of China under grants no. 30325035 and no. U0631008, the National Basic Research Program of China under grant no. 2006CB 101802, the National High Technology Research and Development Program of China (863 Program) under grants no. 2006AA09Z445 and no. 2006AA100309, the Guangdong Province Natural Science Foundation under grant no. 20023002, and the Science and Technology Bureau of Guangdong Province.

We thank JunFeng Xie for supplying the vector pcXGFP, which was used to construct pG48R and pGV121, and ZhenHui Xie, Luo Fang, and Shen Chen for skilled technical assistance.

REFERENCES

1. **Bahary, N., K. Goishi, C. Stuckenholz, G. Weber, J. Leblanc, C. A. Schafer, S. S. Berman, M. Klagsbrun., and L. I. Zon.** 2007. Duplicate VegfA genes and orthologues of the KDR receptor tyrosine kinase family mediate vascular development in the zebrafish. Blood **110:**3627–3636.
2. **Baraban, S. C.** 2007. Emerging epilepsy models: insights from mice, flies, worms and fish. Curr. Opin. Neurol. **20:**164–168.
3. **Berghmans, S., C. Jette, D. Langenau, K. Hsu, R. Stewart, T. Look, and J. P. Kanki.** 2005. Making waves in cancer research: new models in the zebrafish. BioTechniques **39:**227–237.
4. **Carmeliet, P.** 2005. VEGF as a key mediator of angiogenesis in cancer. Oncology **69**(Suppl. 3)**:**4–10.
5. **Chen, X. H., K. B. Lin, and X. W. Wang.** 2003. Outbreaks of an iridovirus disease in maricultured large yellow croaker, Larimichthys crocea (Richardson), in China. J. Fish Dis. **26:**615–619.
6. **Chinchar, V. G., S. Essbauer, J. G. He, A. Hyatt, T. Miyazaki, V. Seligy, and T. Williams.** 2005. Part II. The double stranded DNA viruses, family Iridoviridae, p. 145–162. *In* C. M. Fauquet, M. A. Mayo, J. Maniloff, U. Desselberger, and L. A. Ball (ed.), Virus taxonomy. VIIIth report of the International Committee on Taxonomy of Viruses. Elsevier/Academic Press, London, United Kingdom.
7. **Chou, H. Y., C. C. Hsu, and T. Y. Peng.** 1998. Isolation and characterization of a pathogenic iridovirus from cultured grouper (Epinephelus sp.) in Taiwan. Fish Pathol. **33:**201–206.
8. **Chua, H. C., M. L. Ng, J. J. Woo, and J. Y. Wee.** 1994. Investigation of outbreaks of a novel disease, "sleepy grouper disease," affecting the brownspotted grouper, Epinephelus tauvina Forskal. J. Fish Dis. **17:**417–427.
9. **Danayadol, Y., S. Direkbusarakom, S. Boonyaratpalin, T. Miyazaki, and M. Miyata.** 1996. An outbreak of iridovirus-like infection in brownspotted grouper (Epinephelus malabaracus) cultured in Thailand. AAHRI Newsl. **5:**6.
10. **Darai, G., H. Delius, J. Clark, H. Apfel, P. Schnitzler, and R. M. Flugel.** 1985. Molecular cloning and physical mapping of the genome of fish lymphocystis disease virus. Virology **146:**292–301.
11. **Darai, G., K. Anders, H. G. Koch, H. Delius, H. Gelderblom, C. Samalecos, and R. M. Flugel.** 1983. Analysis of the genome of fish lymphocystis disease virus isolated directly from epidermal tumours of pleuronectes. Virology **126:**466–479.
12. **Delius, H., G. Darai, and R. M. Flugel.** 1984. DNA analysis of insect iridescent virus 6: evidence for circular permutation and terminal redundancy. J. Virol. **49:**609–614.
13. **Deng, M., J. G. He, S. P. Weng, K. Zeng, Z. Zeng, and Q. X. Long.** 2001. Purification and genomic analysis of infectious spleen and kidney necrosis virus (ISKNV) from mandarinfish. J. Fish. China **25:**238–243. (In Chinese with English abstract.)
14. **Deng, M., J. G. He, T. Zuo, S. P. Weng, K. Zeng, and L. Lu.** 2000. Infectious spleen and kidney necrosis virus (ISKNV) from sinipercachuatsi: development of a PCR detection method and the new evidence of iridovirus. Chin. J. Virol. **16:**365–369. (In Chinese with English abstract.)
15. **Eaton, H. E., J. Metcalf, E. Penny, V. Tcherepanov, C. Upton, and C. R. Brunetti.** 2007. Comparative genomic analysis of the family Iridoviridae: re-annotating and defining the core set of iridovirus genes. Virology **4:**11–18.
16. **Ferrara, N.** 2004. Vascular endothelial growth factor: basic science and clinical progress. Endocr. Rev. **25:**581–611.
17. **Ferrara, N., and T. Davis-Smyth.** 1997. The biology of vascular endothelial growth factor. Endocr. Rev. **16:**4–25.
18. **Gille, H., J. Kowalski, B. Li, J. LeCouter, B. Moffat, T. F. Zioncheck, N. Pelletier, and N. Ferrara.** 2001. Analysis of biological effects and signaling properties of Flt-1 (VEGFR-1) and KDR (VEGFR-2). A reassessment using novel receptor-specific vascular endothelial growth factor mutants. J. Biol. Chem. **276:**3222–3230.
19. **Groves, R. W., E. Wilson-Jones, and D. M. MacDonald.** 1991. Human orf and milkers' nodule: a clinicopathologic study. J. Am. Acad. Dermatol. **25:**706–711.
20. **Grozio, A., A. Catassi, Z. Cavalieri, L. Paleari, A. Cesario, and P. Russo.** 2007. Nicotine, lung and cancer. Anticancer Agents Med. Chem. **7:**461–466.
21. **Habeck, H., J. Odenthal, B. Walderich, H. Maischein, S. Schulte-Merker, and Tubingen 2000 Screen Consortium.** 2002. Analysis of a zebrafish VEGF receptor mutant reveals specific disruption of angiogenesis. Curr. Biol. **12:** 1405–1412.
22. **Haig, D. M., and A. A. Mercer.** 1998. Ovine diseases. Orf. Vet. Res. **29:**311–326.
23. **Hammerschmidt, M., G. N. Serbedzija, and A. P. McMahon.** 1996. Genetic analysis of dorsoventral pattern formation in the zebrafish: requirement of a BMP-like ventralizing activity and its dorsal repressor. Genes Dev. **10:**2452–2461.
24. **He, J. G., M. Deng, S. P. Weng, Z. Li, S. Y. Zhou, Q. X. Long, X. Z. Wang, and S. M. Chan.** 2001. Complete genome analysis of the mandarin fish infectious spleen and kidney necrosis iridovirus. Virology **291:**126–139.
25. **He, J. G., K. Zeng, S. P. Weng, and S. M. Chan.** 2002. Experimental transmission, pathogenicity and physical-chemical properties of infectious spleen and kidney necrosis virus (ISKNV). Aquaculture **204:**11–24.
26. **Houck, K. A., N. Ferrara, J. Winer, G. C. Achianes, B. Li., and D. W. Leung.** 1991. The vascular endothelial growth factor family: identification of a fourth molecular species and characterization of alternative splicing of RNA. Mol. Endocrinol. **5:**1806–1814.
27. **Inder, M. K., N. Ueda, A. A. Mercer, S. B. Fleming, and L. M. Wise.** 2007. Bovine papular stomatitis virus encodes a functionally distinct VEGF that binds both VEGFR-1 and VEGFR-2. J. Gen. Virol. **88:**781–791.
28. **Inouye, K., K. Yamano, Y. Maeno, K. Nakajima, M. Matsuoka, Y. Wada, and M. Sorimachi.** 1992. Iridovirus infection of cultured Red Sea bream, Pagrus major. Fish Pathol. **27:**19–27.
29. **Jung, S., T. Miyazaki, M. Miyata, Y. Danayadol, and S. Tanaka.** 1997. Pathogenicity of iridovirus from Japan and Thailand for the Red Sea bream Pagrus major in Japan, and histopathology of experimentally infected fish. Fish. Sci. **63:**735–740.
30. **Jung, S. J., and M. J. Oh.** 2000. Iridovirus-like infection associated with high mortalities of striped beakperch, Oplegnathus fasciatus (Temmink et Schlegel), in southern coastal areas of the Korean peninsula. J. Fish Dis. **23:**223–226.
31. **Keck, P. J., S. D. Hauser, G. Krivi, K. Sanzo, T. Warren, J. Feder, and D. T. Connolly.** 1989. Vascular permeability factor, an endothelial cell mitogen related to platelet derived growth factor. Science **246:**1309–1312.
32. **Kimmel, C. B., W. W. Ballard, S. R. Kimmel, B. Ullmann, and T. F. Schilling.** 1995. Stages of embryonic development of the zebrafish. Dev. Dyn. **203:**253–310.
33. **Lee, P., K. Goishi, A. J. Davidson, R. Mannix, L. Zon, and M. Klagsbrun.** 2002. Neuropilin-1 is required for vascular development and is a mediator of VEGF-dependent angiogenesis in zebrafish. Proc. Natl. Acad. Sci. USA **99:**10470–10475.
34. **Leung, D. W., G. Cachianes, W. J. Kuang, D. V. Goeddel, and N. Ferrara.** 1989. Vascular endothelial growth factor is a secreted angiogenic mitogen. Science **246:**1306–1309.
35. **Liang, D., J. R. Chang, A. J. Chin, A. Smith, C. Kelly, E. S. Weinberg, and R. Ge.** 2001. The role of vascular endothelial growth factor (VEGF) in vasculogenesis, angiogenesis, and hematopoiesis in zebrafish development. Mech. Dev. **108:**29–43.
36. **Liao, W., B. W. Bisgrove, H. Sawyer, B. Hug, B. Bell, K. G. Peters, D. J. Grunwald, and D. Y. R. Stainier.** 1997. The zebrafish gene cloche acts upstream of a flk-1 homologue to regulate endothelial cell differentiation. Development **124:**381–389.
37. **Liu, W., and D. A. Saint.** 2002. A new quantitative method of real time reverse transcription polymerase chain reaction assay based on simulation of polymerase chain reaction kinetics. Anal. Biochem. **302:**52–59.
38. **Lü, L., S. Y. Zhou, C. Chen, S. P. Weng, S. M. Chan, and J. G. He.** 2005. Complete genome sequence analysis of an iridovirus isolated from the orange-spotted grouper, Epinephelus coioides. Virology **339:**81–100.
39. **Lyttle, D. J., K. M. Fraser, S. B. Fleming, A. A. Mercer, and A. J. Robinson.** 1994. Homologs of vascular endothelial growth factor are encoded by the poxvirus orf virus. J. Virol. **68:**84–92.
40. **McColl, B. K., S. A. Stacker, and M. G. Achen.** 2004. Molecular regulation of the VEGF family—inducers of angiogenesis and lymphangiogenesis. APMIS **112:**463–480.
41. **McGrogan, D. G., V. E. Ostland, P. J. Byrne, and H. W. Ferguson.** 1998. Systemic disease involving an iridovirus-like agent in cultured tilapia, Oreochromis niloticus L. J. Fish Dis. **21:**149–152.
42. **Mercer, A., S. Fleming, A. Robinson, P. Nettleton, and H. Reid.** 1997. Molecular genetic analyses of parapoxviruses pathogenic for humans. Arch. Virol. Suppl. **13:**25–34.
43. **Mercer, A. A., L. M. Wise, A. Scagliarini, C. J. McInnes, M. Buettner, H. J. Rhiza, C. A. McCaughan, S. B. Fleming, N. Ueda, and P. F. Nettleton.** 2002. Vascular endothelial growth factors encoded by Orf virus show surprising sequence variation but have a conserved, functionally relevant structure. J. Gen. Virol. **83:**2845–2855.
44. **Meyer, M., M. Clauss, A. Lepple-Wienhues, J. Waltenberger, H. G. Augustin, M. Ziche, C. Lanz, M. Buttner, H. J. Rziha, and C. Dehio.** 1999. A novel vascular endothelial growth factor encoded by Orf virus, VEGF-E, mediates angiogenesis via signalling through VEGFR-2 (KDR) but not VEGFR-1 (Flt-1) receptor tyrosine kinases. EMBO J. **18:**363–374.
45. **Millauer, B., S. Wizigmann-Voos, H. Schnürch, R. Martinez, N. P. Moller, W. Risau, and A. Ullrich.** 1993. High affinity VEGF binding and developmental expression suggest Flk-1 as a major regulator of vasculogenesis and angiogenesis. Cell **72:**835–846.
46. **Moss, B.** 1996. Poxviridae and their replication, p. 2637–2671. *In* B. N. Fields, D. M. Knipe, and P. Howley (ed.), Fields virology, 3rd ed., vol. 2. Lippincott-Raven Publishers, Philadelphia, PA.
47. **Neufeld, G., T. Cohen, S. Gengrinovitch, and Z. Poltorak.** 1999. Vascular endothelial growth factor (VEGF) and its receptors. FASEB J. **13:**9–22.
48. **Ogawa, S., A. Oku, A. Sawano, S. Yamaguchi, Y. Yazaki, and M. Shibuya.** 1998. A novel type of vascular endothelial growth factor, VEGF-E (NZ-7 VEGF), preferentially utilizes KDR/Flk-1 receptor and carries a potent mitotic activity without heparin-binding domain. J. Biol. Chem. **273:**31273–31282.
49. **Otrock, Z. K., J. A. Makarem, and A. I. Shamseddine.** 2007. Vascular

endothelial growth factor family of ligands and receptors: review. Blood Cells Mol. Dis. **38:**258–268.
50. **Page, R. D.** 1996. TreeView: an application to display phylogenetic trees on personal computers. Comput. Appl. Biosci. **12:**357–358.
51. **Quinn, T. P., K. G. Peters, C. De Vries, N. Ferrara, and L. T. Williams.** 1993. Fetal liver kinase 1 is a receptor for vascular endothelial growth factor and is selectively expressed in vascular endothelium. Proc. Natl. Acad. Sci. USA **90:**7533–7537.
52. **Roberts, W. G., and G. Palade.** 1995. Increased microvascular permeability and endothelial fenestration induced by vascular endothelial growth factor. J. Cell Sci. **108:**2369–2379.
53. **Rodge, H. D., M. Kobs, A. Macartney, and G. N. Frerichs.** 1997. Systemic iridovirus infection in freshwater angelfish, Pterophyllum scalare (Lichtenstein). J. Fish Dis. **20:**69–72.
54. **Rottbauer, W., S. Just, G. Wessels, N. Trano, P. Most, H. A. Katus, and M. C. Fishman.** 2005. VEGF-PLCgamma1 pathway controls cardiac contractility in the embryonic heart. Genes Dev. **19:**1624–1634.
55. **Savory, L. J., S. A. Stacker, S. B. Fleming, B. E. Niven, and A. A. Mercer.** 2000. Viral vascular endothelial growth factor plays a critical role in orf virus infection. J. Virol. **74:**10699–10706.
56. **Schulte-Merker, S., R. K. Ho, B. G. Herrmann, and C. Nüsslein-Volhard.** 1992. The protein product of the zebrafish homologue of the mouse T gene is expressed in nuclei of the germ ring and the notochord of the early embryo. Development **116:**1021–1032.
57. **Seiler, C., K. C. Finger-Baier, O. Rinner, Y. V. Makhankov, H. Schwarz, S. C. Neuhauss, and T. Nicolson.** 2005. Duplicated genes with split functions: independent roles of protocadherin 15 orthologues in zebrafish hearing and vision. Development **132:**615–623.
58. **Senger, D. R., S. J. Galli, A. M. Dvorak, C. A. Perruzzi, V. S. Harvey, and H. F. Dvorak.** 1983. Tumor cells secrete a vascular permeability factor that promotes accumulation of ascites fluid. Science **219:**983–985.
59. **Shi, C. Y., Y. G. Wang, S. L. Yang, J. Huang, and Q. Y. Wang.** 2004. The first report of an iridovirus-like gent infection in farmed turbot, Scophthalmus maximus, in China. Aquaculture **236:**11–25.
60. **Shibuya, M.** 2001. Structure and dual function of vascular endothelial growth factor receptor-1 (Flt-1). Int. J. Biochem. Cell Biol. **33:**409–420.
61. **Shibuya, M., and L. Claesson-Welsh.** 2006. Signal transduction by VEGF receptors in regulation of angiogenesis and lymphangiogenesis. Exp. Cell Res. **312:**549–560.
62. **Sollner, C., G. J. Rauch, J. Siemens, R. Geisler, S. C. Schuster, U. Muller, and T. Nicolson.** 2004. Mutations in cadherin 23 affect tip links in zebrafish sensory hair cells. Nature **428:**955–959.
63. **Sudthongkong, C., M. Miyata, and T. Miyazaki.** 2002. Iridovirus disease in two ornamental tropical freshwater fishes: African lampeye and dwarf gourami. Dis. Aquat. Organ. **48:**163–173.
64. **Sudthongkong, C., M. Miyata, and T. Miyazaki.** 2002. Viral DNA sequence of genes encoding the ATPase and the major capsid protein of tropical iridovirus isolates which are pathogenic to fishes in Japan, South China Sea and Southeast Asian countries. Arch. Virol. **147:**2089–2109.
65. **Tidona, C. A., and G. Darai.** 1997. The complete DNA sequence of lymphocystis disease virus. Virology **230:**207–216.
66. **Tischer, E., R. Mitchell, T. Hartmann, M. Silva, D. Gospodarowicz, J. Fiddes, and J. Abraham.** 1991. The human gene for vascular endothelial growth factor. J. Biol. Chem. **266:**11947–11954.
67. **Tokunaga, Y., Y. Yamazaki, and T. Morita.** 2006. Localization of heparin- and neuropilin-1-recognition sites of viral VEGFs. Biochem. Biophys. Res. **348:**957–962.
68. **Ueda, N., L. M. Wise, S. A. Stacker, S. B. Fleming, and A. A. Mercer.** 2003. Pseudocowpox virus encodes a homolog of vascular endothelial growth factor. Virology **305:**298–309.
69. **Ueda, N., M. K. Inder, L. M. Wise, S. B. Fleming, and A. A. Mercer.** 2007. Parapoxvirus of red deer in New Zealand encodes a variant of viral vascular endothelial growth factor. Virus Res. **124:**50–58.
70. **Wang, Y. Q., L. Lu, S. P. Weng, J. N. Huang, S. M. Chan, and J. G. He.** 2007. Molecular epidemiology and phylogenetic analysis of a marine fish infectious spleen and kidney necrosis virus-like (ISKNV-like) virus. Arch. Virol. **152:** 763–773.
71. **Weng, S. P., J. G. He, K. Zeng, Z. J. Huang, K. T. Hou, W. P. Huang, J. H. Chen, and J. R. Luo.** 1998. Infectious spleen and kidney necrosis virus infection in Siniperca chuatsi—histopathology and relationship with HB, RBC and WBC. J. South China Normal Univ. **82:**70–76. (In Chinese with English abstract.)
72. **Wilgus, T. A., A. M. Matthies, K. A. Radek, J. V. Dovi, A. L. Burns, R. Shankar, and L. A. DiPietro.** 2005. Novel function for vascular endothelial growth factor receptor-1 on epidermal keratinocytes. Am. J. Pathol. **167:** 1257–1266.
73. **Williams, T.** 1996. The iridoviruses. Adv. Virus Res. **46:**345–412.
74. **Willis, D. B., and A. Granoff.** 1980. Frog virus 3 DNA is heavily methylated at CpG sequences. Virology **107:**250–257.
75. **Wilting, J., R. Birkenhager, A. Eichmann, H. Kurz, G. Martiny-Baron, D. Marme, J. E. McCarthy, B. Christ, and H. A. Weich.** 1996. VEGF121 induces proliferation of vascular endothelial cells and expression of flk-1 without affecting lymphatic vessels of chorioallantoic membrane. Dev. Biol. **176:**76–85.
76. **Wise, L. M., N. Ueda, N. H. Dryden, S. B. Fleming, C. Caesar, S. Roufail, M. G. Achen, S. A. Stacker, and A. A. Mercer.** 2003. Viral vascular endothelial growth factors vary extensively in amino acid sequence, receptor-binding specificities, and the ability to induce vascular permeability yet are uniformly active mitogens. J. Biol. Chem. **278:**38004–38014.
77. **Wise, L. M., T. Veikkola, A. A. Mercer, L. J. Savory, S. B. Fleming, C. Caesar, A. Vitali, T. Makinen, K. Alitalo, and S. A. Stacker.** 1999. Vascular endothelial growth factor (VEGF)-like protein from orf virus NZ2 binds to VEGFR2 and neuropilin-1. Proc. Natl. Acad. Sci. USA **96:**3071–3076.
78. **Zachary, I.** 2003. VEGF signalling: integration and multitasking in endothelial cell biology. Biochem. Soc. Trans. **31:**1171–1177.